PHYSICAL REVIEW A **70**, 011601(R) (2004)

Faraday patterns in low-dimensional Bose-Einstein condensates

Kestutis Staliunas,[1,*] Stefano Longhi,[2,†] and Germán J. de Valcárcel[3,‡]
[1]*ICREA, Departament de Fisica i Enginyeria Nuclear, Universitat Politecnica de Catalunya, Colom 11, E-08222 Terrassa, Barcelona, Spain*
[2]*INFM, Dipartimento di Fisica and IFN, Politecnico di Milano, Piazza L. da Vinci 32, I-20133 Milano, Italy*
[3]*Departament d'Òptica, Universitat de València, Dr. Moliner 50, E-46100 Burjassot, Spain*
(Received 25 September 2003; published 12 July 2004)

Excitation of Faraday patterns in the *weak* confinement space of low-dimensional Bose-Einstein condensates (BEC) by a periodic modulation of the trap frequency, Ω_{tight}, in the tight confinement space is shown. For slow modulation the low-dimensional dynamics of the BEC in the weak confinement space is described by a Gross-Pitaevskii equation with time modulated nonlinearity coefficient. For increasing modulation frequencies a noticeable reduction of the pattern formation threshold is observed near $2\Omega_{\mathrm{tight}}$, which is related to the parametric excitation of the internal breathing mode in the tight confinement space. These predictions could be relevant for the experimental excitation of Faraday patterns in BEC.

DOI: 10.1103/PhysRevA.70.011601 PACS number(s): 03.75.Hh, 05.45.−a, 47.54.+r

The nonlinear spatiotemporal dynamics of Bose-Einstein condensates (BECs) is attracting increasing interest in recent years, with a major focus toward the conservative dynamics of spatially localized structures like solitons and vortices. The possibility of controlling the evolution of bright and dark solitons or of periodic matter waves has been widely addressed in recent works by exploiting, among others, the temporal modulation of the atomic scattering length [1]. Less attention has been devoted so far to the study of the dynamics of dissipative BECs in view of the potential observation of spatially-extended matter-wave dissipative patterns [2,3] which are ubiquitous in spatially extended physical systems driven far from equilibrium [4]. We recently predicted [3] the spontaneous emergence of patterns and quasipatterns in BECs when the atomic scattering length is periodically modulated in time. As these patterns arise due to the modulation of a system parameter (the scattering length), they show features similar to the parametric Faraday waves observed on the free surface of a fluid subjected to oscillatory vertical acceleration (see, e.g., Ref. [4]). Indeed, the atomic density waves excited in this way oscillate at half the modulation frequency, and the selected wave-number depends on the modulation frequency through a dispersion-induced mechanism.

Here we show that, in low-dimensional BECs, Faraday patterns can be excited by modulating the trap frequency in the tight confinement direction, alternatively to the modulation of the atomic scattering length. This way 2D (1D) Faraday patterns can be excited across the extended dimensions of disk- (cigar-) shaped BECs. We also show that this mechanism introduces new resonance phenomena which yield, among others, to a noticeable lowering of the pattern formation threshold. These results are of major interest for an experimental observation of dissipative patterns in BECs, where modulation of trap frequencies is usually easier than modulation of the atomic scattering length.

The starting point of our analysis is the Gross-Pitaevskii (GP) Eq. (6) for a confined BEC, generalized to include damping [7]:

$$i\hbar\frac{\partial\Psi}{\partial t}=(1-i\gamma)\left(-\frac{\hbar^2}{2m}\nabla^2+V(\mathbf{r},t)+C|\Psi|^2-\bar{\mu}\right)\Psi, \quad (1)$$

where $C=4\pi\hbar^2Na/m$, N is the number of particles, a is the interatomic s-wave scattering length ($a>0$ for a repulsive BEC, which we consider), m is the mass of the particles, $\bar{\mu}$ is the chemical potential, $V(\mathbf{r},t)$ is the trapping potential, and γ is the damping parameter. The phenomenological model of a dissipative BEC described by Eq. (1) is compatible with experiments for dilute alkali BEC near absolute zero, and it has been used by several authors to study, e.g., vortex lattice formation in rotating BECs [8] and splitting of quantized BEC vortices [9]. Estimated values for γ in ^{87}Rb and ^{23}Nd range between 0.005 and 0.03 [7–9]. In the absence of damping the normalization imposes $\int|\Psi(\mathbf{r},t)|^2d^3r=1$. Our study covers both the 1D case of a cigar-shaped BEC extended along the z direction, $V(\mathbf{r},t)=\frac{1}{2}m[\Omega_{\mathrm{tight}}^2(t)(x^2+y^2)+\Omega_{\mathrm{weak}}^2z^2]$, and the 2D case of a disk-shaped BEC extended in the (x,y) plane, $V(\mathbf{r},t)=\frac{1}{2}m[\Omega_{\mathrm{tight}}^2(t)z^2+\Omega_{\mathrm{weak}}^2(x^2+y^2)]$. The condition $\Omega_{\mathrm{weak}}\ll\Omega_{\mathrm{tight}}$ is assumed which means that Ω_{weak} and Ω_{tight} are the frequencies of the trap along the weak and tight confinement directions, respectively. We assume that Ω_{tight} is subjected to periodic modulation: $\Omega_{\mathrm{tight}}(t)=\bar{\Omega}_{\mathrm{tight}}[1+\alpha\cos(\Omega t)]$. In terms of the scaled variables $\tau=\bar{\Omega}_{\mathrm{tight}}t$, $\mathbf{R}\equiv(X,Y,Z)=(x,y,z)/a_{\mathrm{tight}}$, $a_{\mathrm{tight}}=\sqrt{\hbar/(m\bar{\Omega}_{\mathrm{tight}})}$, and $u=a_{\mathrm{tight}}\sqrt{4\pi aN}\Psi$, and assuming for definiteness a disk-shaped BEC, Eq. (1) takes the following dimensionless form:

$$i\frac{\partial u}{\partial\tau}=(1-i\gamma)[-\tfrac{1}{2}\nabla_{\mathbf{R}}^2+\tfrac{1}{2}\omega_{\mathrm{tight}}^2(\tau)Z^2+\tfrac{1}{2}\omega_{\mathrm{weak}}^2(X^2+Y^2)+|u|^2-\mu]u, \quad (2)$$

where

*Electronic address: kestutis.staliunas@icrea.es
†Electronic address: longhi@fisi.polimi.it
‡Electronic address: german.valcarcel@uv.es

$$\omega_{\mathrm{tight}}(\tau) = 1 + \alpha \cos(\omega\tau), \quad (3)$$

$\omega_{\mathrm{weak}} = \Omega_{\mathrm{weak}}/\overline{\Omega}_{\mathrm{tight}} \ll 1$, $\omega = \Omega/\overline{\Omega}_{\mathrm{tight}}$, and $\mu = \overline{\mu}/(\hbar\overline{\Omega}_{\mathrm{tight}})$. The dynamical equation for a cigar-shaped BEC is retrieved from Eq. (2) after interchanging ω_{weak} with ω_{tight}. In the absence of damping the normalization condition for u reads $\int |u(\mathbf{R},\tau)|^2 d^3R = Q$, where $Q = 4\pi Na/a_{\mathrm{tight}}$ is an adimensional parameter characterizing the strength of the nonlinear interaction. Below we show that, for $\omega \ll 1$ (slow modulation), Eq. (2) can be reduced to the same GP equation as used in Ref. [3] to describe Faraday patterns in BECs under scattering length modulation. The physical reason for the equivalence of modulating the scattering length and the trap frequency corresponding to the tightly confined direction (z) lies in the (periodically forced) breathing dynamics of the BEC across that direction. This dynamics entails a periodic change of the BEC density which, in its turn, leads to an effective modulation of the nonlinear particle interaction in the weakly confined (x,y) plane. However, as ω is increased, a resonance phenomenon is observed near $\omega = 2(\Omega = 2\overline{\Omega}_{\mathrm{tight}})$, corresponding to the parametric excitation of the BEC breathing mode in the tight confinement direction [10]. Although close to resonance the dynamics becomes complicated and a reduction to a lower-dimensional GP equation is not possible, pattern formation is still predicted and occurs at much lower thresholds, which may be of major interest from an experimental viewpoint.

We consider first the slow-modulation regime. The reduction of the BEC 3D dynamics to an effective 2D description is done through a multiple scale analysis [11]. We assume a slow modulation, $\omega \propto O(\varepsilon)$ (with $\varepsilon \ll 1$), a weak interaction of particles, $|u|^2 \propto O(\varepsilon)$, and a large $[\propto O(\varepsilon^{-1/2})]$ characteristic spatial scale of the BEC wave function variation across the weak confinement plane. This scaling corresponds to $Q \propto O(\varepsilon^0)$, which is compatible with typical experimental conditions with dilute BECs (see, e.g., [6]). Under these conditions a weakly nonlinear analysis of Eq. (2), which uses $\varepsilon^{1/2}$ as the expansion parameter, leads to the factorization

$$u(X,Y,Z,\tau) = [\tfrac{1}{2}\omega_{\mathrm{tight}}(\tau)]^{1/4}\exp[-\tfrac{1}{2}\omega_{\mathrm{tight}}(\tau)Z^2]\psi(X,Y,\tau), \quad (4)$$

where, at the leading order, the reduced amplitude $\psi \propto O(\varepsilon^{1/2})$ satisfies

$$i\frac{\partial \psi}{\partial \tau} = \frac{1 - i\gamma}{2}[-\nabla^2_{\mathrm{weak}} + \omega^2_{\mathrm{weak}}(X^2 + Y^2) + \sqrt{\omega_{\mathrm{tight}}(\tau)}|\psi|^2 - \mu_1]\psi, \quad (5)$$

which is obtained as a solvability condition at order $\varepsilon^{3/2}$ in the asymptotic expansion. The chemical potential $\mu = [\omega_{\mathrm{tight}}(\tau) + \mu_1]/2$, with $\mu_1 \propto O(\varepsilon)$ [12]. Note that Eq. (5) is a damped GP equation with time-varying nonlinear term. Note also that, for a flat trap in the weakly confined space ($\omega_{\mathrm{weak}} = 0$) and small dissipation coefficient and modulation depth ($\gamma, \alpha \ll 1$), Eq. (5) becomes

a)
b)
c)
d)
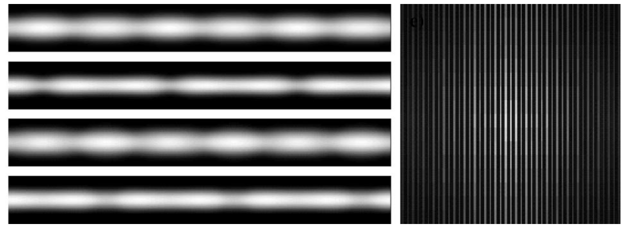

FIG. 1. (a)– (d) Sequence of BEC density as taken at every 1/2 of the trap modulation period (from top to bottom); (e) BEC density in momentum space (density of the spatial Fourier spectrum of the BEC wave function) corresponding to snapshot (a). Plots are obtained by numerical integration of Eq. (2) with periodic boundary conditions in both directions, and with the trapping potential in the vertical (Y) direction. The trap modulation frequency is $\omega = 0.62(\omega_{\mathrm{breath}} \approx 1.77)$. Other parameters are $\alpha = 0.5$, $\gamma = 0.01$, and $\mu = 1.54$. The spatial grid is 256×32 (aspect ratio: 8:1). The size of integration space along the horizontal (X) coordinate is 176. The mode $n = 3$ of periodic boundaries (along the X axis) is excited.

$$2i\frac{\partial \psi}{\partial \tau} = (1 - i\gamma)(-\nabla^2_{\mathrm{weak}} - \mu_1 + |\psi|^2)\psi + \alpha_0\cos(\omega\tau)|\psi|^2\psi, \quad (6)$$

with $\alpha_0 = \alpha/2$ (for cigar-shaped BECs, $\alpha_0 = \alpha$). In its present form Eq. (6) coincides with Eq. (3) in [3], which was shown to support Faraday-type patterns. The wave-number $k = k(\omega)$ of the excited pattern and the threshold $\alpha_{0,\mathrm{thr}}(k)$ for pattern formation at the first parametric resonance tongue follow from Ref. [3]:

$$k(\omega) = \sqrt{-\mu_1 + \sqrt{\mu_1^2 + \omega^2}},$$

$$\alpha_{0,\mathrm{thr}}(k) = \frac{2\gamma\sqrt{2\mu_1 + k^2}(\mu_1 + k^2)}{k}. \quad (7)$$

The behavior predicted by Eqs. (7) was confirmed by a direct numerical integration of Eq. (2). In order to reduce the computational time the simulations were carried out in 2D space by assuming a tight (weak) confinement in the vertical (horizontal) direction. Periodic boundary conditions along the horizontal direction were used, corresponding to the limiting case of flat potential in the elongated direction. Figure 1 shows an example of quasi-1D Faraday patterns. A sequence of snapshots of the BEC density in coordinate space is shown at time intervals equal to half the modulation period (left), and BEC density in momentum space corresponding to snapshot (a) is shown on the right. The BEC density pulsates in the tightly confined (vertical) space at the trap modulation frequency ω, see Eqs. (3) and (4), whereas the BEC spatiotemporal oscillations along the weakly confined space occur at half the trap modulation frequency. Note that the values of the modulation frequency ($\omega = 0.62$) and of the reduced chemical potential ($\mu_1 = 2.08$, as calculated from the value $\mu = 1.54$ used in simulations) are of order of 1. This means that the mechanism of excitation of Faraday patterns is efficient even when the parameters of the system are beyond the smallness assumptions underlying Eq. (5).

RAPID COMMUNICATIONS

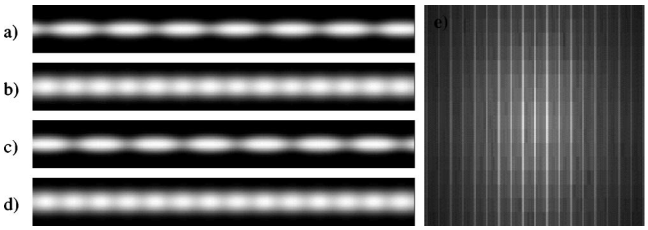

FIG. 2. Same as Fig. 1, except for parameters. The trap modulation frequency $\omega=1.56$ is closer to the frequency of the BEC breathing mode in the vertical direction: $\omega_{\text{breath}}\approx 1.77$; $\alpha=0.1$. The mode $n=6$ of periodic boundaries (along the X axis) is excited.

The parametric excitation process usually saturates for sufficiently large dissipation, leading to a stationary pattern (steadily oscillating with the half of excitation frequency), whereas for very weak damping the direct parametric process can be followed by its inverse process, leading to periodical sequences of revivals similar to those observed in conservative 1D BECs [13]. We observed periodic revivals typically for $\gamma\leqslant 0.001$, whereas damped periodic revivals are obtained for more realistic values of γ (we typically used $\gamma\propto 0.01$ [7–9].

A key aspect of the modulation frequency value used in Fig. 1 is that it is far below the natural oscillation frequency of the BEC breathing mode in the tight confinement direction, ω_{breath}, which is close to 2. As ω is increased close to ω_{breath}, the BEC dynamics becomes more involved owing to the parametric excitation of the internal breathing mode [10]. In the conservative, undriven case such breathing oscillations are undamped [10], and in an elongated BEC may lead to a self-parametric instability, i.e., the transfer of the breathing energy to longitudinal waves in the weak confinement space [14]. In the presence of damping and trap frequency modulation, an enhancement of the breathing oscillation depth is expected when the parametric resonance condition $\omega=\omega_{\text{breath}}$ is attained, with a corresponding threshold lowering for pattern formation. Numerical simulations of Eq. (2) show indeed such a characteristic resonance behavior. As an example, Fig. 2 shows pattern formation dynamics for $\omega=1.54$, which is close to the expected resonance $\omega=\omega_{\text{breath}}\sim 1.77$, which has been numerically computed by perturbing the undriven ground state. The main effect observed, as compared to Fig. 1, is the enhancement of the contrast of the pattern, as well as a dramatic lowering of the pattern formation threshold. In fact the numerically found thresholds are $\alpha_{thr}=0.149$ and $\alpha_{thr}=0.031$ for Figs. 1 and 2, respectively. Figure 3(a) shows the dependence of the numerically determined threshold on the modulation frequency (circles), compared with the theoretical prediction valid for slow modulation, Eq. (7) (dashed line); the wave numbers of the corresponding patterns are shown in Fig. 3(b). Due to periodic boundaries the allowed wave numbers have a discrete character [the set of spatial (Fourier) modes is discrete]. This explains the observed periodic-like character of the pattern formation threshold that lowers for some frequencies (those resonant with BEC modes in the weakly confined direction). The theoretical dashed curve, as expected, does not capture the threshold lowering at $\omega=\omega_{\text{breath}}$, which is due to the enhancement of the BEC breathing in the tightly confined direction. To quantitatively evaluate such a resonance in a simple way, let us assume a BEC with large aspect ratio ($\omega_{\text{weak}}=0$) and use a Gaussian-shaped Ansatz to Eq. (2) disregarding the spatial dynamics in the nonconfined space. We consider a disk-shaped BEC and set $u=A(\tau)\exp[-\beta(\tau)Z^2]$, where $A(\tau)$ and $\beta(\tau)$ are complex-valued functions of time. After substituting the Ansatz into Eq. (2) and making a parabolic approximation in Z of the nonlinear term one obtains:

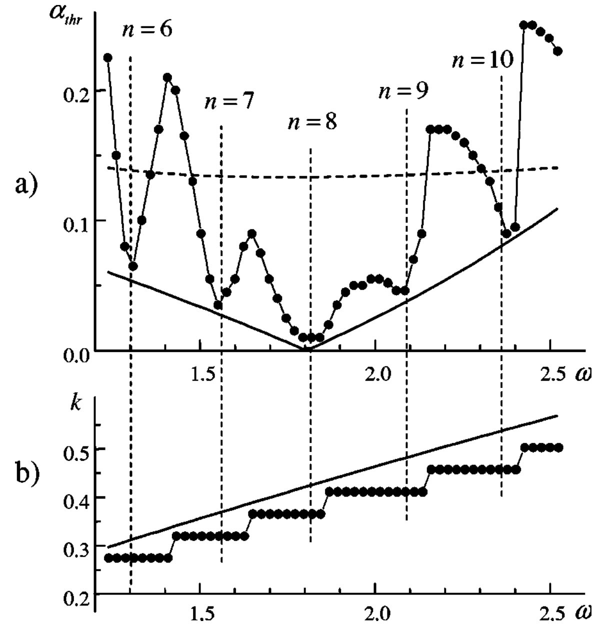

FIG. 3. (a) Pattern formation threshold vs modulation frequency (neutral stability curve) as obtained by numerical integration of Eq. (2) (solid circles), by analytical asymptotic analysis [Eqs. (7), dashed line], and by the analytical model taking into account the resonant enhancement of BEC pulsation [Eqs. (8), solid line]; (b) wave number of the pattern as obtained by numerical integration of Eq. (2) (solid circles), and by the analytical model (line). Parameters and conditions are the same as in Fig. 1.

$$\frac{dA}{d\tau}=-(\gamma+i)(\beta+|A|^2-\mu)A, \tag{8a}$$

$$\frac{d\beta}{d\tau}=-(\gamma+i)[2\beta^2+|A|^2(\beta+\beta^*)-\tfrac{1}{2}\omega_{\text{tight}}^2(\tau)]. \tag{8b}$$

In the absence of modulation [$\omega_{\text{tight}}=1$, Eq. (3)] the steady-state solution to Eqs. (8), which corresponds to the BEC ground state, reads $\overline{\beta}=1/(4\mu)$, $|\overline{A}|^2=\mu-1/(4\mu)$, which imposes $\mu>1/2$. The BEC response for small ω, Eq. (3), is easily studied in the limit $\gamma,\alpha\ll 1$ by standard linearization of Eqs. (8) around the steady state. The expression for the amplitude $\Delta|A|^2$ of the BEC peak density oscillations around its mean value $|\overline{A}|^2$ is too cumbersome to be given here; however simple expressions can be provided for $\gamma\to 0$. For a disk-shaped BEC the resonance frequency is $\omega_{\text{res}}^2=3+1/(4\mu^2)$, which compares well with the numerical result $\omega_{\text{breath}}\approx 1.77$ for the parameters used in Figs. 1 and 2. Note that $\omega_{\text{breath}} \to 2$ when $\mu \to 1/2$, i.e., when $|\overline{A}|^2 \to 0$, which is the noninteraction limit. If we introduce the modulation enhancement factor $\delta = (\Delta|A|^2/|\overline{A}|^2)/\alpha$, in the limit $\gamma \to 0$ one obtains $\delta = 2/|\omega^2 - \omega_{\text{res}}^2|$, which for $\omega \ll \omega_{\text{tight}}$ gets close to $1/2$, i.e., corresponds well to that following from the asymptotic expansion (6): $\alpha_0/\alpha = 1/2$. Analogous calculations for cigar-shaped BECs lead to $\omega_{\text{res}} = 2$, and $\delta = 4/|\omega^2 - \omega_{\text{res}}^2|$ independently of the value of μ, which is compatible with Ref. [10].

The above study has been performed in the zero confinement limit in the weak confinement space. More realistic configurations were considered by numerically integrating Eq. (2) with a weak harmonic potential trap in the weakly confined direction. Figure 4 shows an example. The pattern formation thresholds as well as the emerging wave numbers in the presence of weak confining potentials correspond satisfactorily to those previously obtained in the absence of axial confinement. In the simulations of Fig. 4 the modulation depth parameter was chosen approximately 2 times above its threshold value, and the patterns depicted appeared after 50 periods of the radial trap modulation.

The calculation in Fig. 4 is a 2D analog of a cigar-shape BEC. The parameters used for the calculation, in terms of real physics units, correspond, e.g., to $N = 5 \times 10^5$ atoms of ^{87}Rb in an elongated trap of axial and radial frequencies of 14 and 112 Hz, respectively, which result in a BEC axial and radial size of 100 and 12.5 μm, respectively. These parameters are compatible with Ref. [15]. The corresponding modulation frequencies used in cases (a), (b), and (c) in Fig. 4 correspond to 190, 257, and 370 Hz.

In conclusion, we demonstrated that low- (one- and two-) dimensional Faraday patterns can be parametrically excited in the weak confinement space of BECs by periodic modulation of the trap frequency in the tight confinement space. The reported mechanism is alternative to the scattering length modulation studied in Ref. [1]. Since the modulation of the trap parameter is usually easier than that of the scattering length, and additionally leads to a dramatic threshold reduction due to the excitation of the BEC internal oscillation mode, we envisage that our results can have major importance toward an experimental observation of Faraday patterns in BECs.

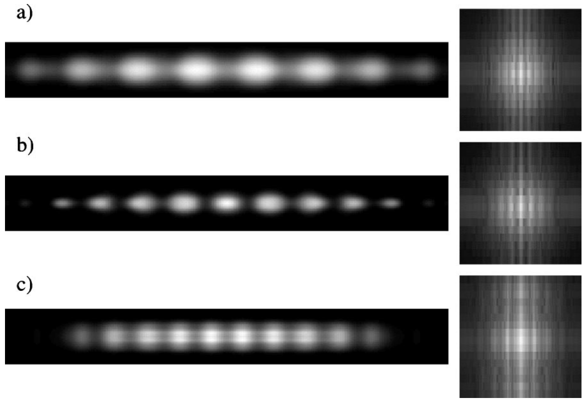

FIG. 4. Snapshots of the BEC density distributions (left, coordinate space; right, momentum space) as obtained by numerical integration of Eq. (2) with the weak (nonzero) confinement potential in the X direction. The aspect ratio of the trap is $\Delta X/\Delta Y \approx 8$. Parameters and conditions as in Fig. 1, and (a) $\omega = 1.55$, $\alpha = 0.15$; (b) $\omega = 2.05$, $\alpha = 0.15$; (c) $\omega = 2.95$, $\alpha = 0.75$.

Financial support from Sonderforschungsbereich 407 of the Deutsche Forschungsgemeinschaft (K.S.) and from the Spanish Ministerio de Ciencia y Tecnología and the European Union FEDER through Project No. BFM2002-04369-C04-01 (G.deV.) is acknowledged. K.S. gratefully acknowledges discussions with M. Lewenstein, L. Santos, and J. Arlt.

[1] H. Saito and M. Ueda, Phys. Rev. Lett. **90**, 040403 (2003); F. Kh. Abdullaev *et al.*, *ibid.* **90**, 230402 (2003); D. E. Pelinovsky, P. G. Kevrekidis, and D. J. Frantzeskakis, *ibid.* **91**, 240201 (2003); F. Kh. Abdullaev *et al.*, Phys. Rev. A **67**, 013605 (2003).
[2] F. T. Arecchi, J. Bragard, and L. M. Castellano, Opt. Commun. **179**, 149 (2000).
[3] K. Staliunas, S. Longhi, and G. J. de Valcárcel, Phys. Rev. Lett. **89**, 210406 (2002).
[4] M. C. Cross and P. C. Hohenberg, Rev. Mod. Phys. **65**, 851 (1993).
[5] S. Inouye *et al.*, Nature (London) **392**, 151 (1998).
[6] F. Dalfovo *et al.*, Rev. Mod. Phys. **71**, 463 (1999).
[7] S. Choi, S. A. Morgan, and K. Burnett Phys. Rev. A **57**, 4057 (1998).
[8] M. Tsubota, K. Kasamatsu, and M. Ueda, Phys. Rev. A **65**, 023603 (2003); K. Kasamatsu, M. Tsubota, and M. Ueda, *ibid.* **67**, 033610 (2003).
[9] M. Möttönen *et al.*, Phys. Rev. A **68**, 023611 (2003).
[10] V. M. Pérez-García *et al.*, Phys. Rev. Lett. **77**, 5320 (1996); J. J. García-Ripoll and V. M. Pérez-García, Phys. Rev. A **59**, 2220 (1999).
[11] V. M. Pérez-García, H. Michinel, and H. Herrero, Phys. Rev. A **57**, 3837 (1998).
[12] For the case of a cigar-shaped BEC, $u = \sqrt{\omega_{\text{tight}}(\tau)} \exp\left[-\frac{1}{2}\omega_{\text{tight}}(\tau)(X^2+Y^2)\right] \psi(Z,\tau)$, $\mu = \omega_{\text{tight}}(\tau) + \mu_1/2$, and $\psi(Z,\tau)$ satisfies Eq. (5) with $\sqrt{\omega_{\text{tight}}(\tau)} \to \omega_{\text{tight}}(\tau)$.
[13] F. Kh. Abdullaev *et al.*, J. Opt. Soc. Am. B **14**, 27 (1997).
[14] Yu. Kagan and L. A. Maksimov, Phys. Rev. A **64**, 053610 (2001).
[15] S. Dettmer *et al.*, Phys. Rev. Lett. **87**, 160406 (2001).